Journal of Electroceramics, 8, 163–174, 2002

Design of and Fabrication Improvements to the Cymbal Transducer Aided by Finite Element Analysis

RICHARD J. MEYER, JR.,[1,*] W. JACK HUGHES,[1] THOMAS C. MONTGOMERY,[1]
DOUGLAS C. MARKLEY[2] & ROBERT E. NEWNHAM[2]

[1]*Applied Research Laboratory, The Pennsylvania State University, State College, PA 16804, USA*
[2]*Materials Research Institute, The Pennsylvania State University, University Park, PA 16804, USA*

Submitted October 12, 2001; Revised May 2, 2002; Accepted July 15, 2002

Abstract. A miniature flextensional transducer, the "cymbal," is an emerging underwater transducer technology for large area and restricted volume transmit and receive arrays. The performance of the device is being evaluated for a number of applications requiring a large number of elements. Simple design, low cost and the ability to tailor performance to the desired application are attractive features of the cymbal. Analysis of the fabrication and performance of the cymbal has revealed that the benefits of the cymbal's flexible design also present production concerns. Asymmetry in the cavity depth or epoxy layer can result in unwanted resonances that can detract from the in-water performance. To avoid these spurious resonances, tolerances in cavity depth could be as low as 5 μm, resulting in low production yields. These and other fabrication concerns have been analyzed through experiment and finite element modeling software using the ATILA code. We were able to identify ways of improving manufacturing yields and minimizing variances to accommodate large array production. The origins of the spurious resonances are discussed along with the performance of a prototype array.

Keywords: transducer, cymbal, flextensional, finite element modeling

Introduction

The "cymbal" transducer is a miniature Class V flextensional transducer developed at the Materials Research Laboratory, Penn State University and patented by Newnham and Dogan in 1998 [1]. The design is an improvement on the commercially successful "moonie" transducer patented by Newnham et al. [2]. The cymbal design stems from stress analysis using finite element software in which inactive cap material was removed from the moonie structure [3]. The names moonie and cymbal come from the crescent cavity shape created by the end cap and the shape of the cap, respectively. The cymbal is a simple version of the ring shell projectors developed by the Defense Research Establishment Atlantic (DREA) in the mid-1970's [4]. The DREA design used a 3-3 mode ceramic ring driver sandwiched between the outer circumference of the radiating shells. Similar to the cymbal and moonie, concave and convex shells were used. The cymbal transducers consist of an electroactive driver sandwiched between two shaped caps as shown in Fig. 1. Moonie and cymbal hydrophones are compact and inexpensive to fabricate and have many potential applications including towed undersea arrays, fish finders, and geophysical research.

Ease of fabrication and the ability to tailor performance to the desired application are attractive features of the cymbal design. In the construction of the moonie, the end caps are machined to the desired cavity depth. For the cymbal, end caps are punched from sheet material or shim stock. Thus, the cymbal is well suited to mass production. The driver material can range from commercially available piezoelectrics and electrostrictors, to ferroelectric phase switchers or even magnetostrictive materials [5]. Common end cap materials used include titanium, brass, kovar, tungsten and steel [6, 7]. The end caps are bonded to the driver using high strength insulating epoxy. The cymbal functions

*To whom all correspondence should be addressed.

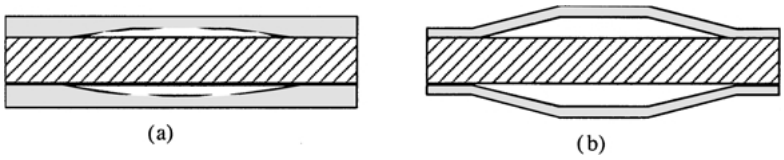

Fig. 1. Schematic structure of (a) moonie and (b) cymbal flextensional transducer. The "driver" (hatched area) and the caps (solid area) have typical dimensions of 12.7 mm in diameter and <3 mm overall thickness. Typical cymbal cap geometrics are: 320 μm cavity depth, 3 mm dome, 250 μm thick caps and a flange width of 1.85 mm.

by adding the radial contraction and thickness expansion of the driver. For piezoceramics, an amplification of the axial motion can be as large as 40 times that of the ceramic alone [5].

The resonance frequency, force, displacement and response time of this structure are controlled through the choice of the cap and driver materials, together with the geometry and overall dimensions. The diameter of the cymbal has the biggest influence on the resonance frequency. By varying the diameter from 40 mm to 3 mm, the resonance frequencies can been tailored from 1 kHz to over 100 kHz. The resonance frequency can also be tailored with changes in cap cavity depth and cap material. Typical cavity depths range from 150 μm to 600 μm. The versatility of the design is well known and has been the topic of many publications [3, 5–9].

As a sound projector or hydrophone, the cymbal transducer is attractive because of its low weight (<2 gms @ 12.7 mm OD), low cost (projected to <$5/unit) and thin profile (<3 mm), which lends itself to large area arrays or restricted volume applications. For underwater applications the cymbal has been tested and modeled as a single element and in arrays [5, 9, 10]. For a typical 12.7 mm (0.5 inch) diameter cymbal with a fundamental resonance around 15 to 20 kHz, the individual cymbal transducer is small compared to the wavelength in water. Consequently, a single cymbal is omnidirectional and it has a very low radiation resistance and a relatively high radiation reactance. Currently, the exact nature of the acoustical impedance load for a cymbal is unknown. The characteristics of the cymbal most likely fall between that of a free pulsating sphere and that of a piston vibrating in free space. This topic will be addressed in future studies. Because of the cymbal's small size, the resulting transfer of radiated acoustic power is reduced due to the mass loading effect. Increasing the radiating area by assembling them into arrays will increase the radiation loading. For low frequency projector applications large area arrays will be necessary to achieve the desired source level and bandwidth requirements [7, 11–13].

Uniformity from element to element is an important aspect of defining mutual interaction and array loading conditions, even more so when the array element spacing is close-packed. To define the behavior of these elements in a large array application, both the amplitude of vibrations and resonance frequency must be controlled. Once this behavior is known, the drive waveform can be conditioned spatially to form the desired acoustic beam. Non-uniformity in resonance frequency may reduce mutual interaction effects but may hinder the ability to form or steer beams.

Typically, a nine-element array is tested as a measure of the performance of a particular cymbal design. For frequencies near 15 kHz, this array is still small compared to the wavelength. To characterize the cymbal performance, evaluate the radiation impedance and mutual interaction as a function of radiating area, and demonstrate beam steering abilities, a large area array is desired. In this study an array of 200 elements was selected, with each cymbal wired individually. To fabricate an array of this size, the production of the cymbals and the method for assembling the array must be carefully analyzed.

This paper describes methods for increased production and handling of cymbal elements for the fabrication of large area arrays. Finite element modeling was used as a tool to analyze the cymbal structure while manufacturing methods were altered to improve production and handling. The effects of bonding and cap variability are described as well as the performance of the newly designed element.

Fabrication Issues

Cymbal prototype fabrication consisted of stamping and shaping the caps using a hardened steel die set. The flange of the end caps was then hand polished to remove

metal burrs and to prepare the surface for bonding. The bonding epoxy, Emerson and Cumming 45 LV Black, was painted onto the flange of the cap. The caps were cemented to the ceramic and clamping rings were used to apply pressure to the flange during the epoxy curing process. For small quantities this hand fabrication process was adequate. However, larger scale production techniques are required to reduce labor cost and improve reproducibility.

Quality control for the finished units involves measuring the electrical impedance spectrum to identify the resonance frequencies. For hand fabrication, a large number of cymbals were observed to have split fundamental flextensional peaks. The characteristics of the split peaks differ for different cymbal diameters. Depicted in Fig. 2(a) and (b) are the measured in-air admittance spectra from a 12.7 mm diameter cymbal and a 15.9 mm diameter cymbal, respectively. In the case of the 12.7 mm diameter cymbal, the secondary peak shows up after the main resonance. The respective positions were reversed for the 15.9 mm diameter cymbal where the first peak was smaller in amplitude than the second peak, indicating a geometrical influence of this behavior. Cymbals containing double peaks were rejected and rebuilt using new caps. Initially, poor bonding was assumed to be the cause of this splitting since hand painting was prone to width and thickness variations. The production yields for acceptable single peak samples made by hand were often as low as 20% and 10% for the 12.7 mm and 15.9 mm diameter cymbals, respectively.

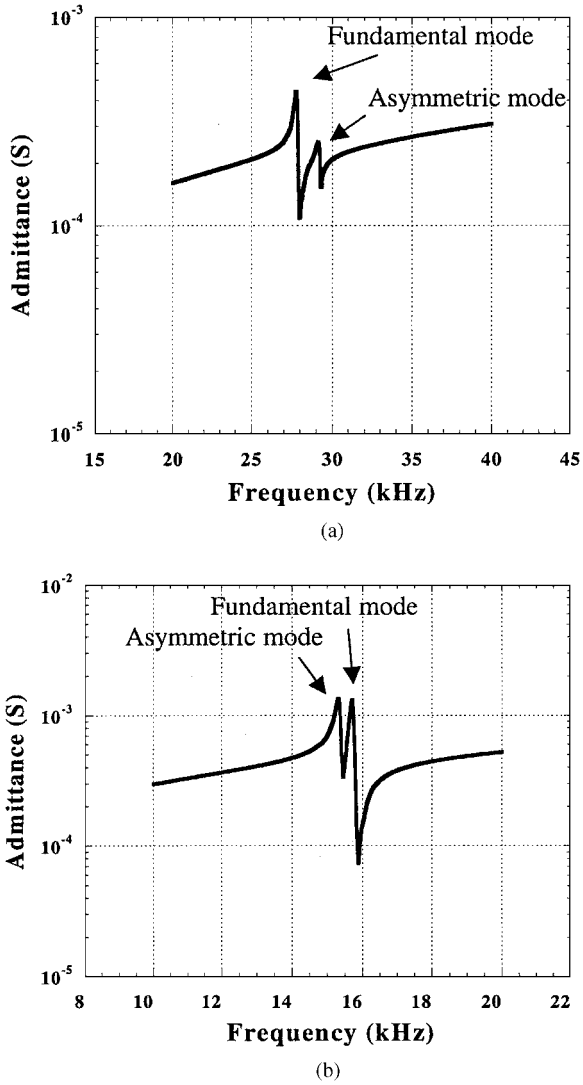

Fig. 2. Measured in-air admittance as a function of frequency for (a) 12.7 mm diameter cymbal and (b) 15.9 mm diameter cymbal.

Modeling Details

Finite element modeling was used to examine the cymbal to understand the nature of the split peaks. The modeling was carried out using the ATILA2D finite element code, and included both modal and harmonic analysis. Using the electrical boundary conditions on the piezoelectric elements, the ATILA code solves the matrix (Eq. (1)) for the eigenvalues under short circuit (resonance modes) and open circuit (antiresonance) conditions. The effective coupling coefficient of the mode was calculated from the resulting resonance and antiresonance frequencies.

$$\begin{bmatrix} [K_{uu}] - \omega^2[M] & [K_{u\Phi}] \\ [K_{u\Phi}]^T & [K_{\Phi\Phi}] \end{bmatrix} \begin{bmatrix} \underline{U} \\ \underline{\Phi} \end{bmatrix} = \begin{bmatrix} \underline{0} \\ -\underline{q} \end{bmatrix} \quad (1)$$

$[K_{uu}]$ = stiffness matrix; $[K_{u\Phi}]$ = piezoelectric matrix; ω = angular frequency; $[K_{\Phi\Phi}]$ = dielectric matrix; $[M]$ = consistent mass matrix; $\underline{U}$ = displacement field vector values; $\underline{\Phi}$ = electrical potential vector values; q = vector values of electrical charges.

A 2D axi-symmetric model was used. The mesh used for in-air analysis is shown in Fig. 3. Half of the cymbal was modeled in order to change the dimensions of the cap from one side to the other. Variables that were considered included cavity depth, epoxy width, and epoxy thickness differences from one side to the

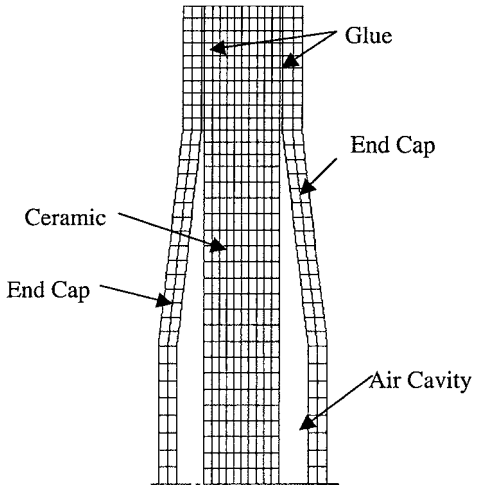

Fig. 3. Two-dimensional axi-symmetric ATILA finite element mesh used for in-air calculations of the cymbal structure.

other. The base model consisted of PZT 5H ceramic of 1 mm thickness, 250 μm thick titanium end caps with 150 μm cavity depth, and a 40 μm thick epoxy bond. The response of the baseline model was consistent with measurements and the admittance spectrum as shown in Fig. 4.

Simulation Results

Initially a change in epoxy thickness was investigated. This was performed by making the epoxy layer on

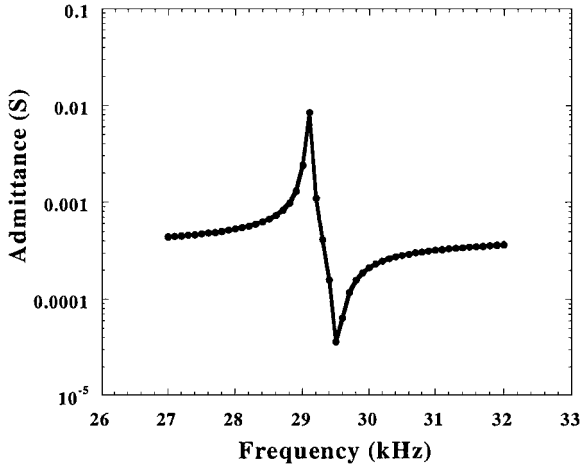

Fig. 4. Calculated admittance spectrum for an axi-symmetric model of the cymbal structure.

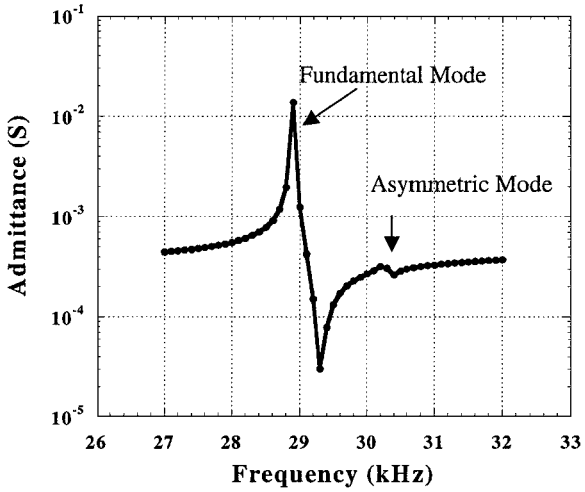

Fig. 5. Calculated admittance spectrum of the cymbal with a difference of only 10 μm in epoxy layer thickness from one side to the other.

the right side of the cymbal thinner than on the left side. Figure 5 shows the in-air admittance of the modeled cymbal with an epoxy thickness difference of only 10 μm. As can be seen, a small secondary peak emerged from the background because of the asymmetry in the epoxy layer. The modes of vibration were analyzed to determine the origin of the second peak. Figure 6 shows the displacements associated with each vibration mode. The fundamental mode (0, 1) and the harmonic mode (0, 2) of the cap were present in all the models. However, an asymmetric mode and a large bending mode were also found when differences were added to the structure. In the asymmetric mode, both caps move in the same direction. This motion included a small bending or buckling motion of the ceramic. The next higher resonance that appeared was due to a bending resonance. Both of these modes arose from the differences in the mechanical clamping conditions from one side to the other.

The epoxy layer thickness was varied up to a 20 μm difference. A plot of the fundamental resonance frequency and the effective coupling coefficient is shown in Fig. 7. These values are plotted for the asymmetric mode and the bending mode resonance in Figs. 8 and 9, respectively. The fundamental mode resonance frequency remained relatively constant, however the effective coupling coefficient of the fundamental mode decreased as the difference in epoxy layer thickness increased. This loss in coupling resulted from energy transferred to the asymmetric and bending modes. As

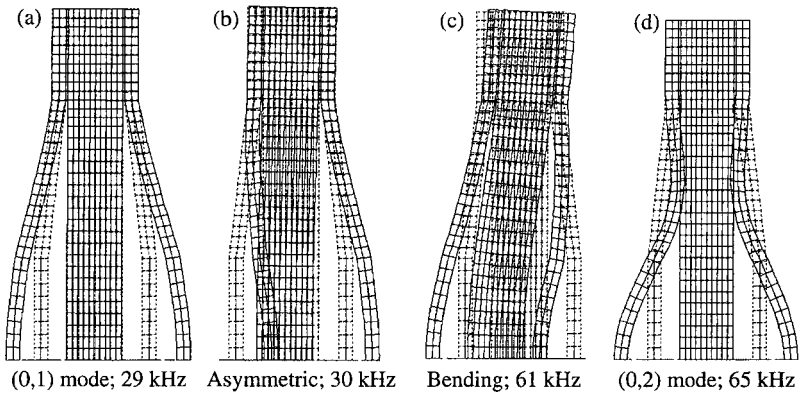

Fig. 6. Finite element modeling of the vibration modes found in the asymmetric cymbal structure together with their corresponding resonance frequencies.

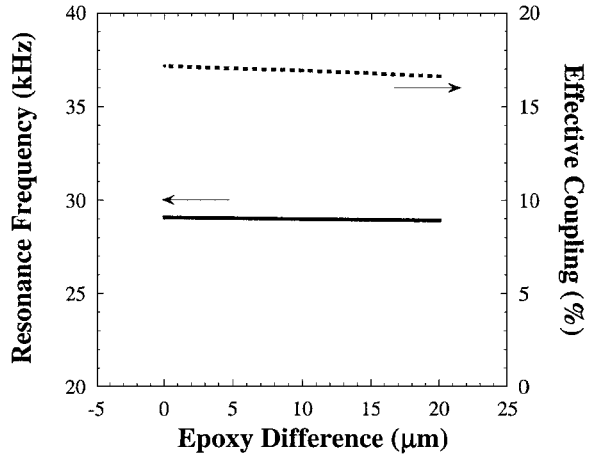

Fig. 7. Fundamental resonance frequency and effective coupling coefficient plotted as a function of epoxy layer difference.

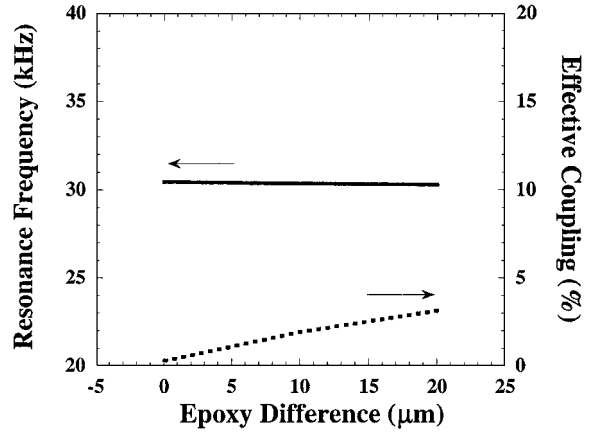

Fig. 8. Asymmetric mode resonance frequency and effective coupling coefficient plotted as a function of epoxy thickness difference.

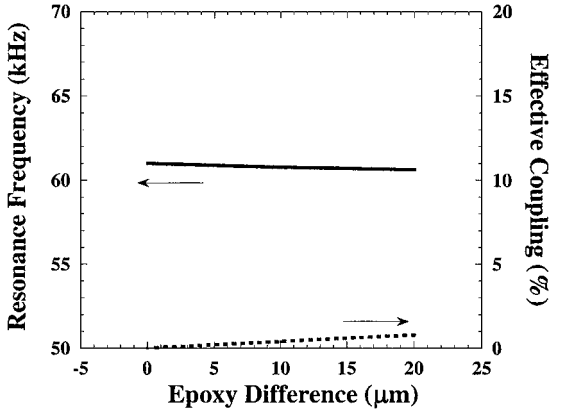

Fig. 9. Ceramic bending mode resonance frequency and coupling coefficient plotted as a function of epoxy thickness difference.

expected, the effective coupling coefficient increased for the asymmetric mode to approximately 3% and the ceramic bending mode coupling increased to almost 1% at the 20 μm epoxy difference.

Another type of asymmetry involves variations in cavity depth from one side of the cymbal to the other. The effect of cavity depth asymmetry was much more pronounced than the epoxy asymmetry. The fundamental resonance behavior was similar to that shown in Fig. 7, but the increase in coupling of the asymmetric mode was much larger. As shown in Fig. 10, with just a 20 μm difference in cavity depth, the coupling coefficient rose to 7%. Harmonic analysis of the 20 μm cavity depth variation was carried out to determine the shape of the admittance curve. The result is shown in Fig. 11. The asymmetric second resonance mode was

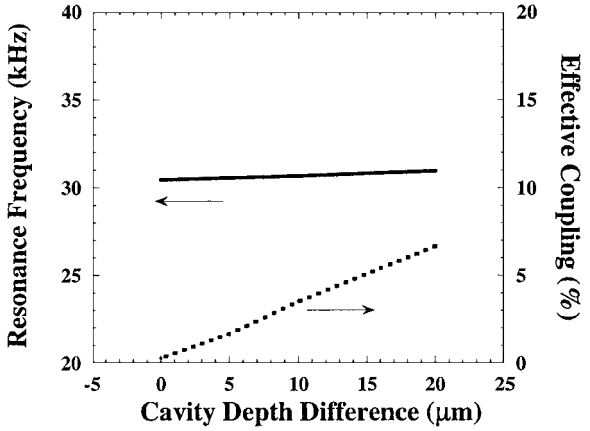

Fig. 10. Asymmetric mode resonance frequency and effective coupling coefficient plotted as a function of cavity depth difference.

clearly seen in the admittance spectrum and occurred at a higher frequency, nearly identical to that observed in the measured values.

The epoxy and cavity depth differences are causing the asymmetric modes to be excited. When resonances are superimposed, the effective coupling of the desired vibration mode is affected. Reduced coupling has a direct effect on the operating bandwidth of the device. In addition, abnormal stresses may be introduced to the ceramic. In either case degraded performance is to be avoided.

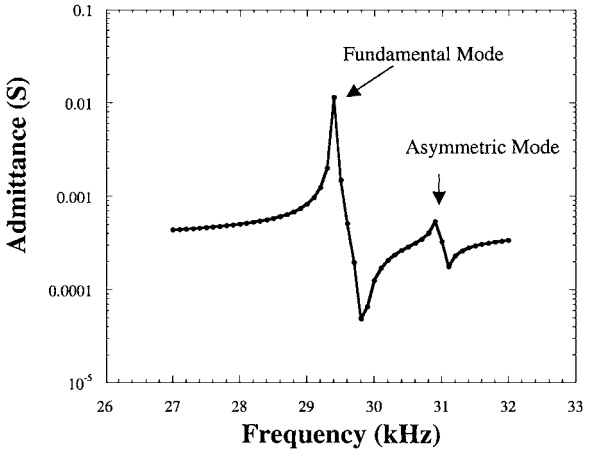

Fig. 11. Calculated admittance spectrum of the cymbal with a cavity depth difference of 20 μm from one side to the other.

Geometry Dependence

The fact that the unwanted asymmetric peak occurs at lower frequencies for 12.7 mm diameter cymbals and at higher frequencies for 15.9 mm diameter cymbals than the major peak suggests that this phenomenon has a geometry dependence. Several ATILA models were generated to observe the resonance frequency of the fundamental and asymmetric modes, as well as the effective coupling coefficients, as a function of cavity depth for the 12.7 mm diameter cymbal. Figure 12

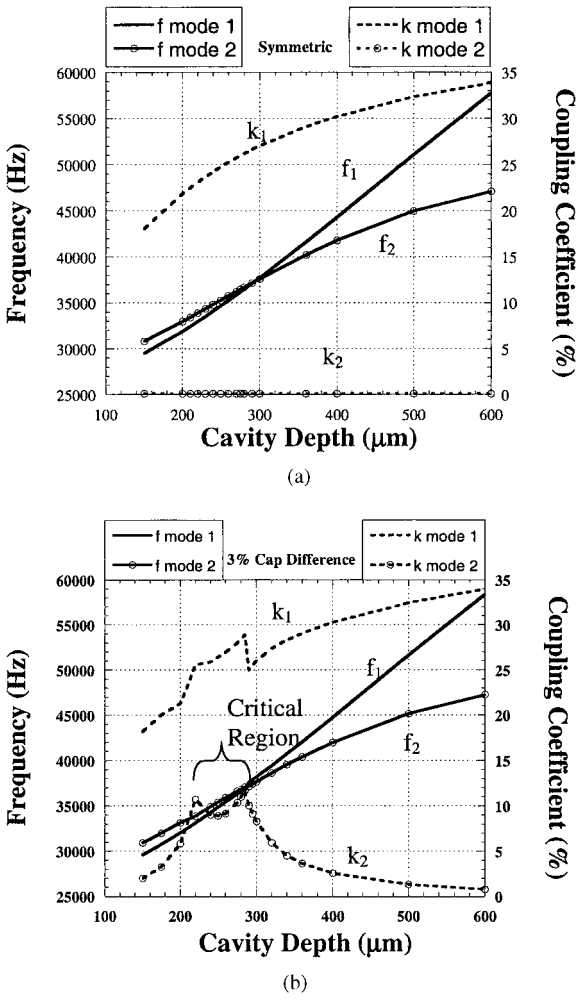

Fig. 12. Resonance frequency and effective coupling coefficient for the fundamental flexural mode (mode 1) and the asymmetric mode (mode 2) plotted as a function of cavity depth for a 12.7 mm diameter cymbal with (a) symmetric capping and (b) 3% variation in cavity depth from one side to the other.

shows the resonance frequency and effective coupling coefficient for the fundamental flexure mode (mode 1) and the asymmetric mode (mode 2) as calculated using modal analysis.

For a symmetrically capped cymbal, Fig. 12(a), the resonance frequency of the fundamental mode and asymmetric mode crossed over at a cavity depth of 290 μm. Thus, the minor or secondary asymmetric resonance can exist at higher or lower frequencies depending on geometry. For ideally symmetric geometry, the asymmetric mode was not electrically coupled but was a mathematical vibration solution of the modal analysis. The coupling coefficient (k_{eff}) for the fundamental mode increased from 18% to 34% for cavity depths of 150 μm to 600 μm, respectively. This increase resulted from more efficient use of the ceramic radial displacement as the flextensional mode moves closer to the ceramic radial resonance, which is 180 kHz for a 12.7 mm disk.

Next, an asymmetry in cap cavity depth of 3% was added to the cymbal calculation. These data are plotted in Fig. 12(b). An electrically coupled asymmetric mode was present over the entire range of cavity depths. The effective coupling coefficient for this mode increased dramatically when its resonance frequency approached that of the fundamental flexural mode. Because of this strong interaction, the coupling coefficient of the fundamental mode also departed from the expected curve.

Differences in the stress distribution from one side of the cymbal to the other, which occur at the hinge point of the flange and the cap cone, are thought to be the origin of the asymmetric mode. These stresses cause a coupling of energy into the disk buckling vibration mode, which is a natural structural resonance. An ATILA calculation showed that, in addition to the electrically coupled radial mode at 180 kHz, a structural resonance of a free 12.7 mm diameter, 1 mm thick, PZT 5H disk occurred at 45 kHz and was not electrically coupled to the applied field. Adding clamping conditions to the disk at the location of the hinge point of the flange resulted in a decrease of this structural resonance to 39 kHz. The clamped disk was still not electrically coupled. The proximity of this natural structural resonance and the flextensional resonance of the caps, corresponding to cavity depths from 220 to 300 μm in Fig. 12(b), results in a "critical region." Critical regions have been defined in other resonator types as well. For example, a vibrating cylinder has a critical region near a length to mean diameter ratio of 1.5:1, where the radial mode and length extensional mode interfere causing a drop in receive sensitivity [14]. For the cymbal, the asymmetric mode shape caused by the buckling of the piezoelectric disk results in a change of phase of the caps. This change in phase occurs as one surface expands while the other contracts; thus, the two caps move in the same direction partially canceling the desired flexural motion.

These curves also suggest that the fabrication tolerance in the cap or bonding dimensions is highly influenced by the proximity of the fundamental and asymmetric modes. For the 12.7 mm size, assuming other geometrical factors remain the same, the yield for fabricating acceptable samples should increase for cavity depths away from the crossover region. If the crossover point occurs at a frequency of interest, the asymmetric mode can be moved to higher or lower resonance frequencies by changing the thickness of the ceramic disk. For a free PZT 5H disk 12.7 mm in diameter and 2 mm in thickness, the structural resonance occurs at 65.5 kHz, 20 kHz higher than the 1 mm thick disk.

Experimental Verification

To confirm the nature of the troublesome asymmetric mode, the vibration velocities of two cymbals were measured. One cymbal displayed multiple resonances in the admittance spectrum and the other a single resonance. The vibration mode was observed as a function of frequency driven at 1 V_{rms} using two laser Doppler vibrometers illuminating opposite faces of the cymbal. The magnitude and phase of the vibrations were recorded with the aid of a computer interface. The cymbals were held in place using spring-loaded supports anchored to the flange.

The results of the laser vibrometer measurements are shown in Figs. 13 and 14 for the multiple and single resonances, respectively. The electrical admittance magnitude and phase, Fig. 13(a), clearly showed the presence of two distinct resonance modes, one at 27.7 kHz and the other at 29.5 kHz. These frequencies corresponded to the maxima in vibration velocity for each cap, as seen in Fig. 13(b). The relative phase between the two laser vibrometers (referenced to the input voltage trigger) is also shown in the Fig. 13(b). The velocity phase measurement has an error of $\pm 5^\circ$. A velocity phase angle of 0° represents the volume expansion and contraction of the caps associated with the fundamental flexure mode as in Fig. 6(a). Caps

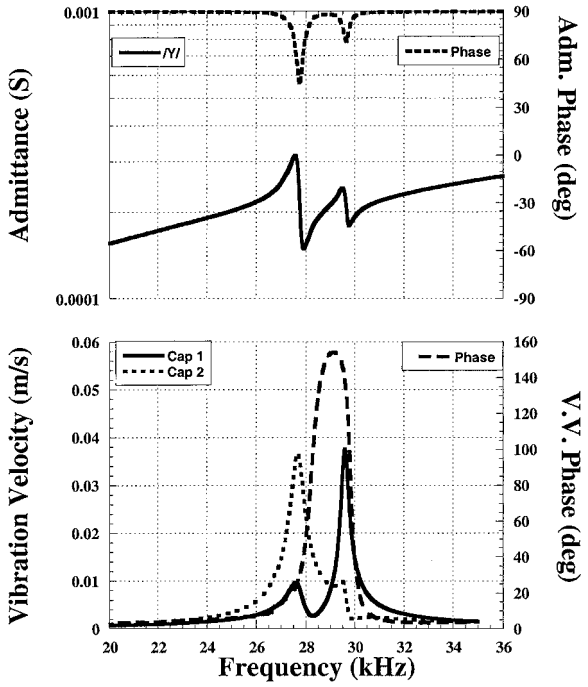

Fig. 13. Admittance magnitude and phase, vibration velocity, and phase of the relative motion of the vibration surfaces of a cymbal plotted as a function of frequency for a sample showing split resonance peaks. The symmetric flexure mode is centered at 27.7 kHz and the interfering asymmetric mode at 29.5 kHz.

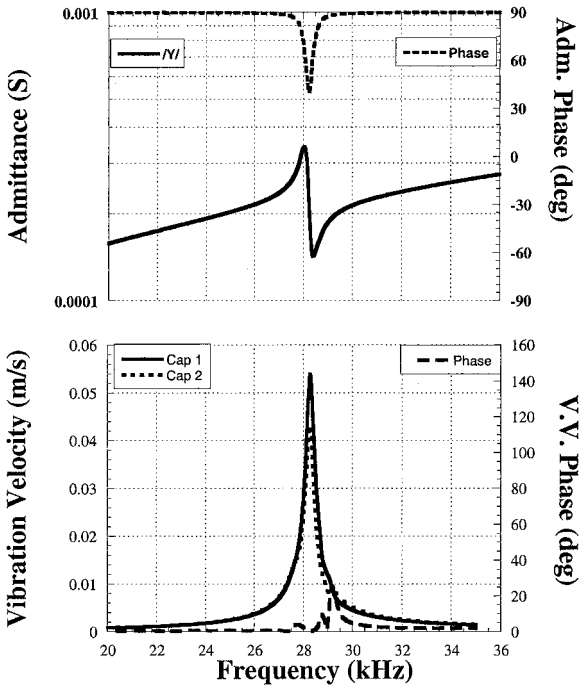

Fig. 14. Admittance magnitude and phase, vibration velocity, and phase of the relative motion of the vibration surfaces of a cymbal plotted as a function of frequency for a sample showing a single resonance peak.

moving in the same direction would have a velocity phase of 180° as in Fig. 6(b). Above the first cap resonance, a measurable change in phase was observed, representing the asymmetric mode predicted by computer modeling. In this particular case, even though the caps are moving out of phase at 29.5 kHz, the contribution of the second cap to the overall displacement was rather small due to its low velocity at that frequency.

Figure 14 illustrates an acceptable sample with only one peak in the admittance spectrum. The two caps were found to have indentical resonance frequencies and slightly different cap vibration velocity magnitudes. Since the measurements were made in-air and the mechanical quality factor (Q_m) of the cymbals is large, it was not unexpected that a difference in cap velocities occurred. The magnitudes of the velocity were higher than observed for the split peak sample. Above the fundamental resonance of 28.2 kHz, a change in phase of up to 30° was measured at 29 kHz. This indicated that the asymmetric mode was present to a small degree even in a cymbal that was thought to be symmetric. The fact that the two caps had the same mechanical resonance but different velocities suggested that a simple impedance measurement might not be sufficient for quality control.

Ramifications of In-Water Operation

Experimental evidence and modeling predictions of the asymmetric mode emphasizes the importance of controlling the fabrication process for building cymbals. Asymmetric modes of vibration detract from the total displacement and therefore the radiation potential of the structure. To predict the effects of asymmetry on the performance of the cymbal in water, the appropriate boundary conditions were added to the models. It is important to note that the water provides a mass and dissipative load. As such the fundamental resonance drops from 28 kHz to 16.5 kHz in-water. The asymmetrical resonance also drops in frequency, however not by the same percentage. Harmonic analysis showed the presence of a dip in the transmit voltage response just above the resonance frequency. Earlier measurements made

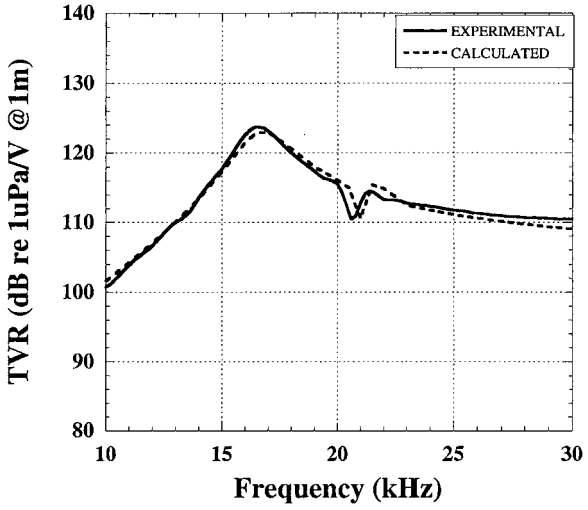

Fig. 15. Transmit voltage response plotted as a function of frequency showing the effect of asymmetry on the measured and modeled in water performance of a single cymbal. [Measured values taken from Ref. [6]].

on a single cymbal element showed a similar dip in the response just above resonance. Previously the dip in performance had been attributed to air bubbles in the urethane waterproofing [7]. Figure 15 shows a comparison of these data to an in-water model. The model accurately predicts the response when asymmetry is added to the geometry. We have concluded that asymmetry is more likely the cause than air bubbles.

Assembly and Wiring Issues

Another troublesome issue for fabricating and testing of the cymbal elements is making good electrical connection to the silvered PZT disks. In the past, electrical leads were attached to the cymbal cap using a silver epoxy bond because solder melting temperatures were above the operating temperature of the cap bonding epoxy. Two problems resulted from this technique: the cymbal and wires must be held until the silver epoxy cures, and good electrical contact between the caps and ceramic electrode is not always achieved. From a practical standpoint, wiring a large area array with conductive epoxy is time consuming and labor intensive. Solder techniques are much more attractive for wiring a large number of elements. In either case, special care must be taken in bonding or soldering to certain cap materials, such as brass or titanium.

A high strength epoxy is used for cap bonding because of the large forces involved in transferring the radial strain of the ceramic to the flexing cap, especially under high drive conditions. Conductive adhesives were shown to fail during drive level testing [7]. The majority of high strength epoxies were electrically insulating, including the one used here. This sometimes leads to a large voltage drop across the bonding layer that can reduce the receive sensitivity of a single element by 14 dB at resonance [7].

Scaling Production

Analysis of the fabrication methods and the performance of the cymbal has identified several production concerns. Small changes in the cavity depth can tune the resonance frequency by several kilohertz to customize the design to specific applications, but, small changes in uniformity can also result in the excitation of unwanted modes of vibration that detract from the performance of the device. For the present design, these tolerances are in the range of only a few micrometers. The analysis has also led to several design and production changes that will improve reproducibility and increase yield. As described previously, cap and bonding uniformity along with wiring and assembly techniques are issues that must be addressed. The next section describes these changes and their impact on the performance and reproducibility of the cymbal transducer.

Modeling and test measurements on the cymbal provide insight into ways to improve large scale production techniques. The first issue addressed was the wiring and connection problem. The goal was to build a large area array in which all the elements were wired individually. The logistics of the wiring resulted in the need to solder the leads while continuing the use of the high strength, insulating epoxy for bonding the caps to the ceramic. Therefore, direct contact to the ceramic electrode was required. ATILA was used to devise a geometry such that exposed the ceramic electrode by simply reducing the flange width. The revised cap geometry is shown in Fig. 16. A 1 mm (0.040 inch) rim was sufficient to accommodate the electrical leads. The old and new style caps were tested for resonance frequency and quasi-static actuator displacement. No differences were observed in performance.

The soldering procedure developed for attaching the wires made use of a low temperature solder (approximately 120°C) from the Indium Corporation of

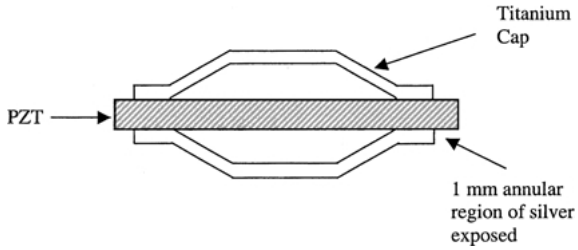

Fig. 16. Schematic of the reduced cap geometry that allowed direct lead connection to the ceramic electrode.

America (Utica, NY). Indalloy® #2 and #8 were effective when used with a low temperature activated flux to solder the leads to the ceramic electrode. Peel tests were carried out to ensure the strength of the solder joint.

To further facilitate production, a new method was devised for applying the epoxy bonding layer. From the modeling results, it was apparent that a very uniform bonding layer is required to obtain a pure flexural mode of the cymbal. Screen-printing was chosen as a production technique of proven reliability capable of controlling the thickness and width of the epoxy. For laboratory production a small hand operated screen with a sample holder mounted on an x, y, z sample stage was constructed. The screen was 130 mm $\times$ 130 mm, 90° 325-mesh, with 12 μm emulsion layer. The screen and sample holder were designed to accommodate two cymbals at a time, with the holder capable of handling either a disk or a cymbal while maintaining the same distance to the screen. The alignment and distance from the sample to the screen could be adjusted using micrometers. A photograph of the laboratory scale screen printer is shown in Fig. 17. Each cymbal was prepared by screening and capping the ceramic disk and then screening and capping the opposite side, and then clamping the structure to cure the epoxy. Should further control or larger production capacity be needed, automated screen printers have an accuracy of less than 1 μm and can accommodate many samples simultaneously.

For clamping and centering the smaller caps during the epoxy curing process, a small "V-block" was built along with aluminum spacer rings that had a cutout to center the cap and apply pressure to only the flange. Pressure was applied to the cymbals during the curing process using a calibrated spring to maintain uniformity.

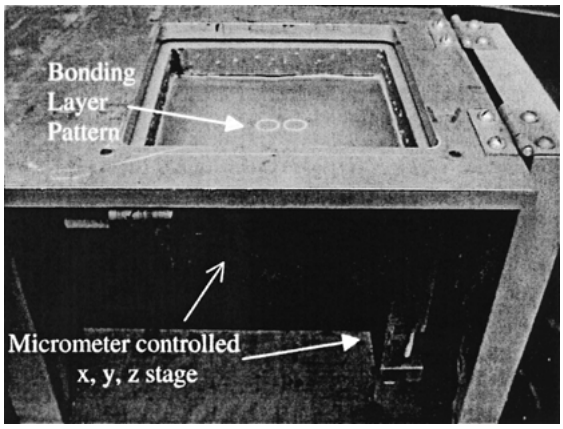

Fig. 17. Photograph of the screen printer showing the micrometer controlled sample stage and the epoxy layer pattern for bonding the caps to the ceramic disk.

To construct a 204-element array and several smaller test arrays, 230 elements were manufactured. The yield of these 12.7 mm diameter cymbals was improved over the hand fabrication processes (20% yield) but was still only 35%. The low yield was attributed to the continued use of the manual punch and forming die set. This process still involved hand shaping and polishing to remove metal burrs and it was difficult to maintain the tight tolerances necessary to produce symmetrically capped samples. Metal stamping technologies could greatly improve fabrication of the metal caps. These technologies can produce large quantities for little expense over the tooling costs.

Array Prototype

A nine-element cymbal array, shown in Fig. 18, was fabricated using Piezo-Kinetics, Inc., PKI-402 ceramic (PZT 4; Navy Type I), 1 mm in thickness and 12.7 mm in diameter. Flextensional caps were shaped from titanium, 250 μm in thickness, to a 150 μm cavity depth. The caps were 11.4 mm in diameter leaving a ceramic edge for solder connection of leads. The caps were bonded using Emerson and Cumming 45 LV black insulating epoxy and cured under compression at 70°C for 4 hours. The elements were wired in parallel in a row/column arrangement and encapsulated in Conathane EN-9 polyurethane (Cytec Industries Inc.) with a 15 mm center-to-center spacing. En-9 is a common urethane used to waterproof forward looking and

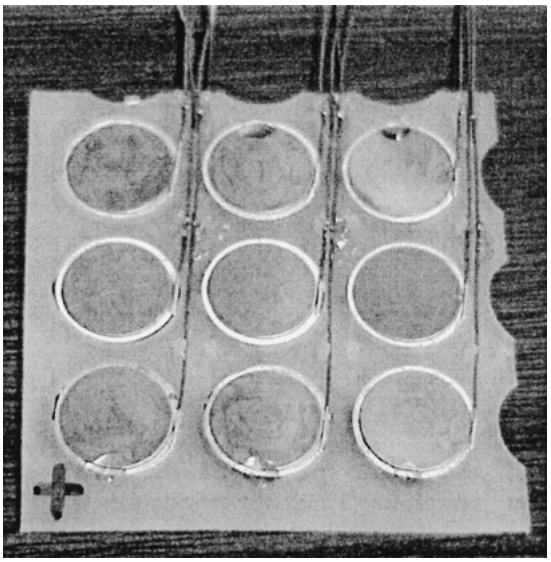

Fig. 18. Nine-element prototype array showing the cymbals wired in a urethane web. Each cymbal is 12.7 mm in diameter.

side scan sonar arrays. The performance of the cymbal array will decrease less than 2 dB over the performance in an oil-filled environment where there are no clamping effects. The loss in performance is outweighed by the ease in design, low cost and better handling ability. Next, the array was mounted and tested in an anechoic test tank. Beam patterns were taken at 8, 15, 30, 45, 60, 80, and 100 kHz to estimate a directivity index. Transmit voltage response (TVR), efficiency (Eff), and impedance magnitude ($|Z|$) and phase were obtained at frequencies from 5 to 100 kHz.

Figures 19 to 21 show the results of the underwater tests. The TVR around the fundamental flextensional resonance of 15 kHz was 124 dB (re: 1 μPa/V @ 1m) with an efficiency near 40%, as shown in Figs. 19 and 20, respectively. A dip in the TVR response was observed from 60 to 70 kHz. This frequency is close to the $(0, 2)$ flextensional mode of the cap in which portions of the cap vibrate out of phase. The TVR remains high at the upper frequencies because of the increase in conductance (G) as the ceramic approaches the radial mode and from an increase in directivity. The magnitude and phase of the impedance is shown in Fig. 21. As can be seen from this plot, the array is essentially a capacitor with the reactance dominating around the mechanical resonance. The performance of the new cap design was identical to the old design.

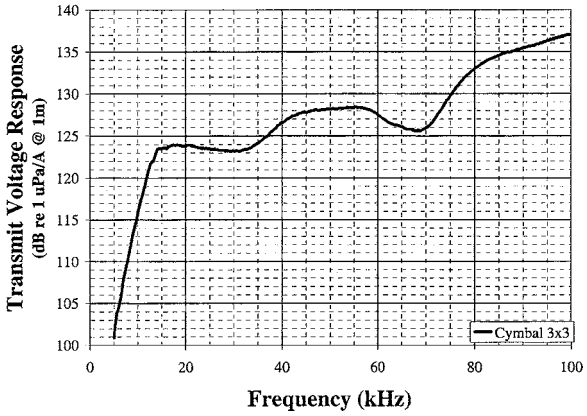

Fig. 19. TVR of a nine-element cymbal array.

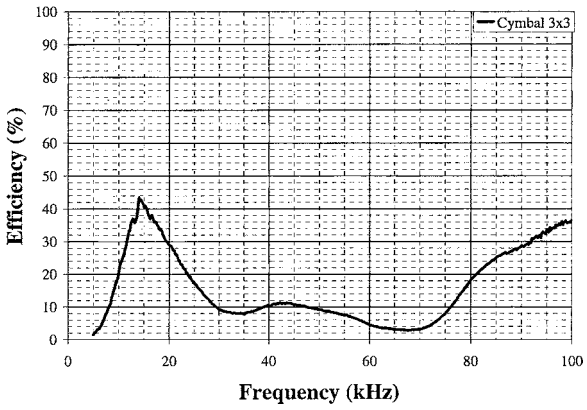

Fig. 20. Efficiency of a nine-element cymbal array.

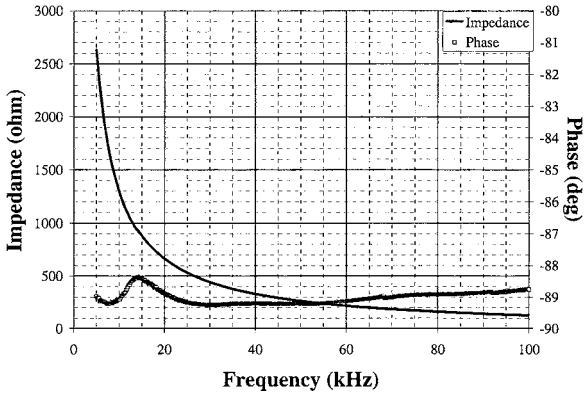

Fig. 21. Impedance magnitude and phase of a nine-element cymbal array.

Conclusions

From a fabrication standpoint, the Class V Flextensional cymbal transducer presents production concerns. It was shown that small variations in epoxy bonding and cap geometry can induce an asymmetric mode, which detracts from the performance of the cymbal. Geometry dependence and alternate methods for avoiding this resonance were presented. The easiest design change to improve production yields and avoid unwanted resonances appears to be to increase the thickness of the ceramic driver. Production yields were improved by using a more controllable method for applying the bonding layer. These thick film techniques are scalable for large production runs. The design modifications were analyzed in a prototype array in the water. The performance of the array was acceptable and production of a large area test array is commencing.

Acknowledgments

The authors would like to thank Bob Dashem and Greg Granville at ARL for production and testing of cymbal arrays; Wipha Yimnirun and Joe Kearns at MRI for cymbal fabrication; Gaylord Shawver, Chris Jabco and Dick Brenneman at MRI for machining and tooling; Shashank Priya for the laser vibrometer measurements; Philippe Bouchilloux at Magsoft for ATILA support; and Tim Meyer at Piezo-Kinetics for expediting our ceramic order. This report was based upon work sponsored by Mr. Les Jecobi, Code 333, Office of Naval Research.

References

1. A. Dogan and R. Newnham, U.S. Patent 5,729,077 (1998).
2. R.E. Newnham, Q.C. Xu, and S. Yoshikawa, U.S. Patent 4,999,819 (1991).
3. A. Dogan, K. Uchino, and R.E. Newnham, *IEEE Transactions on Ultrasonics, Ferroelectrics, and Frequency Control*, **44**(3), 597 (1997).
4. G.W. McMahon, in *Proceedings of the International Workshop on Power Transducers for Sonics and Ultrasonics* (Springer-Verlag, Berlin, 1990), p. 60.
5. R.J. Meyer, Jr. and R.E. Newnham, *Journal of Intelligent Materials Systems and Structures*, **11**, 199 (2001).
6. J.F. Tressler, W. Cao, K. Uchino, and R.E. Newnham, *IEEE Transactions on Ultrasonics, Ferroelectrics, and Frequency Control*, **45**(5), 1367 (1998).
7. J. Zhang, W. Jack Hughes, R.J. Meyer Jr., K. Uchino, and R.E. Newnham, *Ultrasonics*, **37**(8), 523 (2000).
8. J.F. Fernandez, A. Dogan, J.T. Fielding, K. Uchino, and R.E. Newnham, *Sensors and Actuators A*, **65**, 228 (1998).
9. R.J. Meyer, Jr., A. Dogan, C. Yoon, S. Pilgrim, and R.E. Newnham, *Sensors and Actuators A*, **87**, 157 (2001).
10. J. Zhang, A.C. Hladky-Hennion, W.J. Hughes, R.J. Meyer, Jr., and R.E. Newnham, *Ultrasonics*, **39**, 91 (2001).
11. J. Zhang, A.C. Hladky-Hennion, W.J. Hughes, R.J. Meyer, Jr., and R.E. Newnham, *IEEE Transactions on Ultrasonics, Ferroelectrics, and Frequency Control*, **48**(2), 560 (2001).
12. R.E. Newnham, S. Alkoy, A.C. Hladky-Hannion, W.J. Hughes, R. Meyer, Jr., D. Markley, and J. Zhang, in *Oceans '01 MTS/IEEE Conference Proceedings* (MTS/IEEE, New York, 2001), vol. 3, p. 1529.
13. W.L. Carney, T.R. Howarth, and J.F. Tressler, on *Oceans '01 MTS/IEEE Conference Proceedings* (MTS/IEEE, New York, 2001), vol. 3, p. 1577.
14. T.F. Hueter and R.H. Bolt, *SONICS* (John Wiley and Sons, New York, 1955), p. 148.